

Molecular physiological characterization of the dynamics of persister formation in *Staphylococcus aureus*

Shiqi Liu,¹ Yixuan Huang,² Sean Jensen,¹ Paul Laman,¹ Gertjan Kramer,² Sebastian A. J. Zaai,³ Stanley Brul¹

AUTHOR AFFILIATIONS See affiliation list on p. 19.

ABSTRACT Bacteria possess the ability to enter a growth-arrested state known as persistence in order to survive antibiotic exposure. Clinically, persisters are regarded as the main causative agents for chronic and recurrent infectious diseases. To combat this antibiotic-tolerant population, a better understanding of the molecular physiology of persisters is required. In this study, we collected samples at different stages of the biphasic kill curve to reveal the dynamics of the cellular molecular changes that occur in the process of persister formation. After exposure to antibiotics with different modes of action, namely, vancomycin and enrofloxacin, similar persister levels were obtained. Both shared and distinct stress responses were enriched for the respective persister populations. However, the dynamics of the presence of proteins linked to the persister phenotype throughout the biphasic kill curve and the molecular profiles in a stable persistent population did show large differences, depending on the antibiotic used. This suggests that persisters at the molecular level are highly stress specific, emphasizing the importance of characterizing persisters generated under different stress conditions. Additionally, although generated persisters exhibited cross-tolerance toward tested antibiotics, combined therapies were demonstrated to be a promising approach to reduce persister levels. In conclusion, this investigation sheds light on the stress-specific nature of persisters, highlighting the necessity of tailored treatment approaches and the potential of combined therapy.

KEYWORDS antibiotic persistence, *Staphylococcus aureus*, proteomics, metabolomics

Antibiotic persistence (hereinafter referred to as persistence), a non-inheritable antibiotic-tolerant growth-arrested phenotype, has been confirmed as the major cause of recurrent and chronic infections, as well as one of the main contributors to the development antibiotic resistance (1, 2). Persisters were firstly discovered in *Staphylococcus aureus* populations as early as in 1942 (3) and are now found in almost all tested bacterial species (4). When exposed to antimicrobials, a tolerant subpopulation that can easily resuscitate back to normal cells with culturability and virulence after stress removal is named persisters, causing recurrent infection during treatment gaps. Thus, a better understanding of the molecular physiology of persisters is expected to contribute to solving these issues.

However, despite the severe impact of persisters and the value of knowing the mechanisms of their formation, this phenotype is still puzzling. The complexity and contradictory information on persisters have been discussed in terms of their high phenotypic heterogeneity (4–6), the variety of mechanisms leading to their generation (7–9), and sometimes the lack of a uniform definition of persisters (10). Regardless of the these challenges, experimentally, a biphasic kill curve is a widely agreed hallmark of persistence (11). During a high-concentration antibiotic treatment, the death of most susceptible cells results in a rapid drop in the curve regarded as phase I, followed by the survival of non-dividing persisters, indicated as phase II, the survivor plateau.

Editor Benjamin P. Howden, The Peter Doherty Institute for Infection and Immunity, Melbourne, Victoria, Australia

Address correspondence to Stanley Brul, s.brul@uva.nl.

Sebastian A. J. Zaai and Stanley Brul contributed equally to this article. These author names appear in order of increasing seniority.

The authors declare no conflict of interest.

See the funding table on p. 19.

Received 29 June 2023

Accepted 24 October 2023

Published 5 December 2023

Copyright © 2023 American Society for Microbiology. All Rights Reserved.

In the present work, *Staphylococcus aureus*, one of the most widespread Gram-positive infectious agents and most frequent pathogen causing chronic disease, was used. By sampling at different time points of the biphasic kill curve, we studied the molecular characteristics of vancomycin or enrofloxacin-treated persistent population at the protein and metabolite levels, by proteome and metabolome analysis, respectively. Vancomycin is a glycopeptide antibiotic that is clinically used as a primary antibiotic of choice against gram-positive pathogens, including *S. aureus*. It inhibits the elongation and cross-linking of peptidoglycan, causing a perturbed cell wall and eventually cell death (12). Enrofloxacin, on the other hand, is a third-generation fluoroquinolone antibiotic that inhibits DNA synthesis via targeting type II DNA gyrase and type IV topoisomerase (13). It is the first fluoroquinolone of choice in veterinary medicine for numerous diseases including *S. aureus* mastitis (14).

Under vancomycin or enrofloxacin exposure, our tested *S. aureus* cultures displayed a similar biphasic kill curve. In the stable persistent population, proteomics data show several common alterations in carbon metabolism, cell wall biosynthesis, and the expression of ribosomal proteins. However, dynamic analysis revealed that there were major differences between the two antibiotic-exposed groups. Moreover, specific molecular pathways were also found to be related to vancomycin or enrofloxacin treatment. In summary, our study highlights the generic molecular physiological makeup of persisters in *S. aureus* that were triggered by two types of antibiotic stresses. At the same time, our findings demonstrate that stress responses are highly antibiotic specific, and not all persisters exhibit identical molecular and physiological features. These results have important implications for developing treatments for persisters, as targeting the specifically upregulated processes by an antibiotic may be pursued in the requirement for complementary approaches with other antibiotics that can act synergistically in inhibiting persister formation.

RESULTS

To identify the proper sampling time points representing the progress of persister formation, a time-kill kinetics assay was conducted under the exposure of vancomycin or enrofloxacin (Fig. 1A). Biphasic killing curves showed two phases: a quick kill (phase I) that lasted for 3–4 hours and the subsequent plateau (phase II) indicating the persistent population. Within the biphasic kill curve, 24-hour treated samples were considered as stable persistent populations (hereinafter referred to as V-24h and E-24h). Vancomycin and enrofloxacin caused similar kill curves, and no significant difference was found between the survival fractions in V-24h and E-24h. The proportion of persisters in V-24h and E-24h was detected through flow cytometry (15). Moreover, around 75% of the detected events represented persisters (Fig. 1B), suggesting that persisters are the major population in the 24-hour antibiotic-treated samples.

Proteome profile dynamics during the generation of persistence

For proteomics, 15 optical density units (15OD) of cell culture were sampled at 1, 4, and 24 hours of antibiotic exposure, representing the beginning of the fast kill process and the beginning and the end of persistent population formation, respectively. 15OD of an early log phase culture was used as control. In total, 21 samples, being 7 treatment groups with 3 replicates of each group, were harvested. Overall, 765 identified proteins present in at least two replicates in at least one group were analyzed for a general quality assessment. The average coefficient of variation of each treatment was below 3% (Fig. 1C), demonstrating a high quantitative reproducibility between biological triplicates. We identified 546 proteins in V-24h and 588 proteins in E-24h. Compared with 450 proteins in control cells, the Venn diagram (Fig. 1D) shows that vancomycin and enrofloxacin exposure triggered 157 and 194 newly synthesized proteins, respectively, among which 115 proteins were common in both V-24h and E-24h samples.

After 24-hour vancomycin exposure, 42 expressed proteins specific for this treatment were enriched and categorized in five metabolic pathways: citrate cycle, peptidoglycan

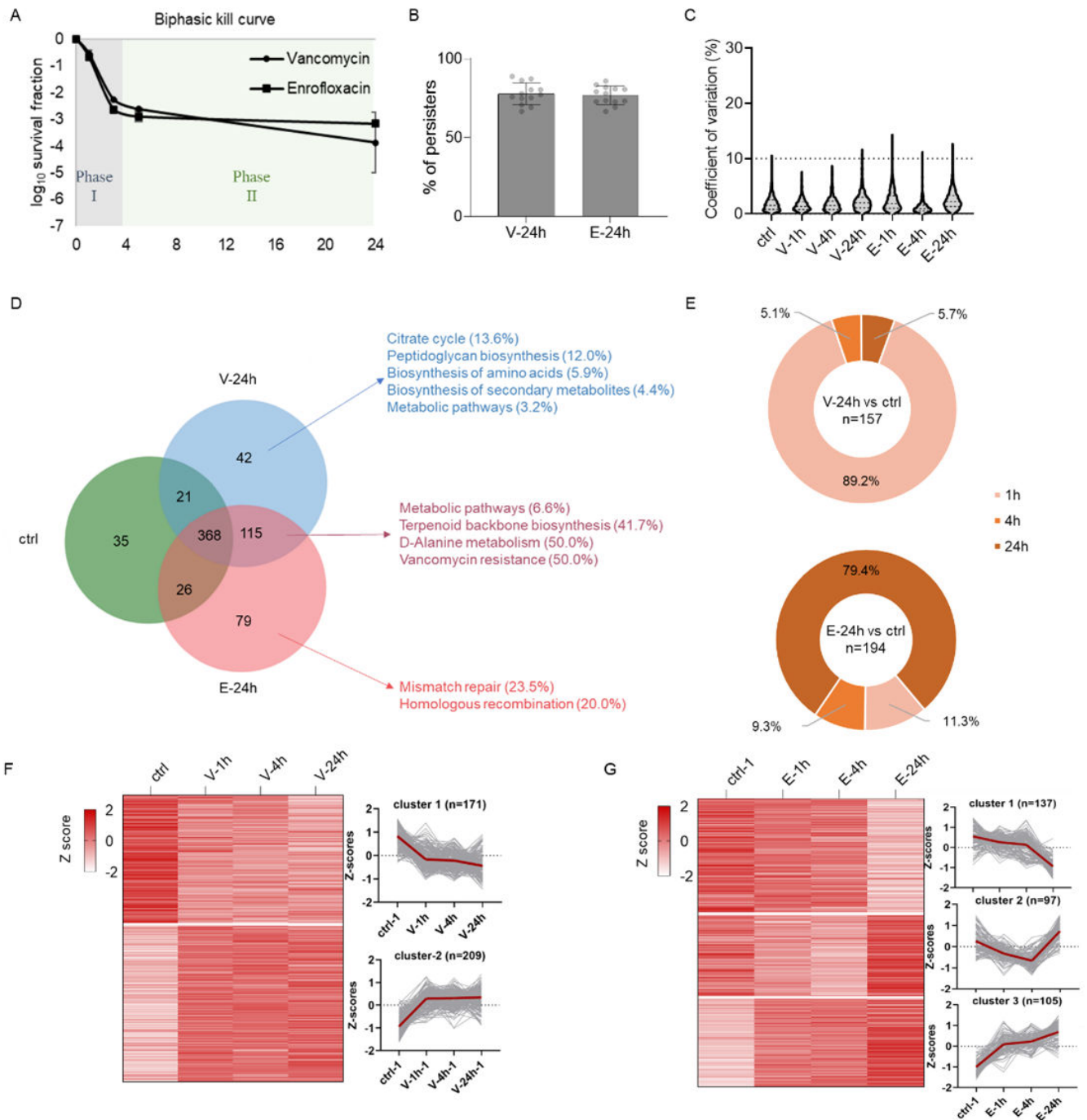


FIG 1 Sample characterization and unique proteome in persistent populations. (A) Time-kill kinetics assay results in biphasic kill curves demonstrating persister formation in a *Staphylococcus aureus* population during 24 hours of antibiotic exposure. Specifically, in phase I, both antibiotics quickly killed around 99.9% of cells after 3–4 hours, leaving behind unsusceptible persisters after phase II. At least three biological replicates were used and the data are shown as mean \pm SD. (B) 5 - (and - 6) - Carboxyfluorescein diacetate that labels metabolically active cells and propidium iodide double staining and subsequent flow cytometry analysis show that, in 24-hour-treated samples, the majority of the cells (~75%) are persisters (CFDA⁺-PI⁻ cells). (C) Fifteen optical density units of cell culture before and after 1-, 4- and 24-hour antibiotic exposure was sampled for proteome analysis. The coefficients of variation of detected proteins between biological triplicates indicate high quantitative reproducibility. (D) Venn diagram of identified proteins from control (ctrl) (green), V-24h (blue), and E-24h (red), as well as enriched Kyoto Encyclopedia of Genes and Genomes pathways. Enrichment factors (“identified protein numbers annotated in this pathway term”/“all protein numbers annotated in this pathway term”) were shown for accumulated pathways. (E) The present proportion of newly synthesized proteins in V-24h and E-24h compared with the untreated control at each time point. For the expression dynamics among proteins that were constitutively expressed, hierarchical cluster analysis was performed with vancomycin-treated samples (F) and enrofloxacin-treated samples (G). The average values are shown for each protein.

biosynthesis, biosynthesis of amino acids, biosynthesis of secondary metabolites, and metabolic pathways. Of these, dihydrolipoyl dehydrogenase, citrate synthase (CitZ), and fumarase (FumC) involved in the tricarboxylic acid (TCA) cycle were detected and are discussed in the next section. Peptidoglycan biosynthesis suggests a protective stress response toward this cell wall-targeting antibiotic. Among 115 proteins shared by the vancomycin- and enrofloxacin-exposed cells, three pathways that are included in cell wall biosynthesis were enriched, suggesting that cell wall alteration can be a general stress response against antibiotics despite a different primary mode of action of antibiotics. Among 72 unique differentially expressed proteins in E-24h, 2 DNA repair-related Kyoto Encyclopedia of Genes and Genomes (KEGG) pathways, mismatch repair and homologous recombination, were enriched. Both of these pathways have been found essential for bacteria to survive under quinolone-induced stress conditions to combat accumulated DNA damage (16–18).

Aside from the mentioned KEGG pathways, we also observed the distinctive expression of a RelA_SpoT domain-containing protein (Q2G2L7) in V-24h, which likely leads to the generation of more (P)ppGpp. This molecule triggers the stringent response, known to contribute to the formation of antibiotic persisters (8). Moreover, six ATP-binding cassette (ABC) transporters were identified in E-24h. ABC transporters are related to transmembrane transport, potentially involved in the efflux of antibiotics. The expression of genes encoding ABC transporters has also been found to be upregulated in intracellular *S. aureus* persisters surviving inside human macrophages (19).

To understand the dynamics of the unique proteome composition under the two different stress conditions, we timed the emergence of the newly synthesized proteins during the biphasic kill curve (Fig. 1E). Interestingly, under vancomycin treatment, 89.2% of these proteins were observed within the first hour of exposure, and only 5.7% after 4 hours of exposure, showing a quick response upon vancomycin-induced stress perception. In contrast, in enrofloxacin-treated cultures, 11.3% of proteins were present at the beginning of antimicrobial exposure, but almost 80% of the induced proteins were only expressed after 4 hours of exposure. Similarly, hierarchical cluster analysis classified two and three clusters with distinct expression patterns from vancomycin-treated samples (Fig. 1F) and enrofloxacin-treated samples (Fig. 1G), respectively. Overall, these findings suggest that the proteome composition is altered differently in the response to the tested stress conditions, where vancomycin tends to cause quick proteome changes within 1 hour of treatment, but where most changes in enrofloxacin-treated samples happen after 4 hours of exposure.

Next, we analyzed 368 commonly expressed proteins in control, V-24h, and E-24h. Compared to untreated control samples, vancomycin induced 44 proteins and repressed 44 proteins (Fig. 2A). In comparison, enrofloxacin caused the overexpression of 65 proteins and the repression of 49 proteins (Fig. 2B). The top 10 predominant proteins in each category were labeled and listed in Table 1, colored in red and green, respectively. In V-24h, highly overexpressed proteins are mainly related to chaperone function (ClpB, GroEL, DnaK, and DnaJ), cell wall biosynthesis (VraR and MurA), and cell membrane regulation functions (branched-chain-amino-acid aminotransferase and acetyl-CoA acyltransferase). In E-24h, most induced proteins engage in DNA repair (UvrABC system protein A, DNA polymerase III, polydeoxyribonucleotide synthase, rNDP, and dCMP kinase) and chaperone function (ClpB, trigger factor). In contrast, most listed decreased proteins in both treated groups were translation related and included ribosomal proteins. KEGG enrichment analysis of differentially expressed proteins revealed five pathways in V-24 (Fig. 2C): ribosome, metabolic pathway, carbon metabolism, biosynthesis of antibiotics, and fatty acid metabolism. In E-24h (Fig. 2D), altered pathways from 114 proteins are related to translation, carbon metabolism, biosynthesis of secondary metabolites, and DNA repair involved pathways nucleotide excision repair and mismatch repair.

Overall, the listed proteome composition illustrates that the alteration in chaperone, carbon metabolism, cell wall biosynthesis, as well as ribosomes are common features

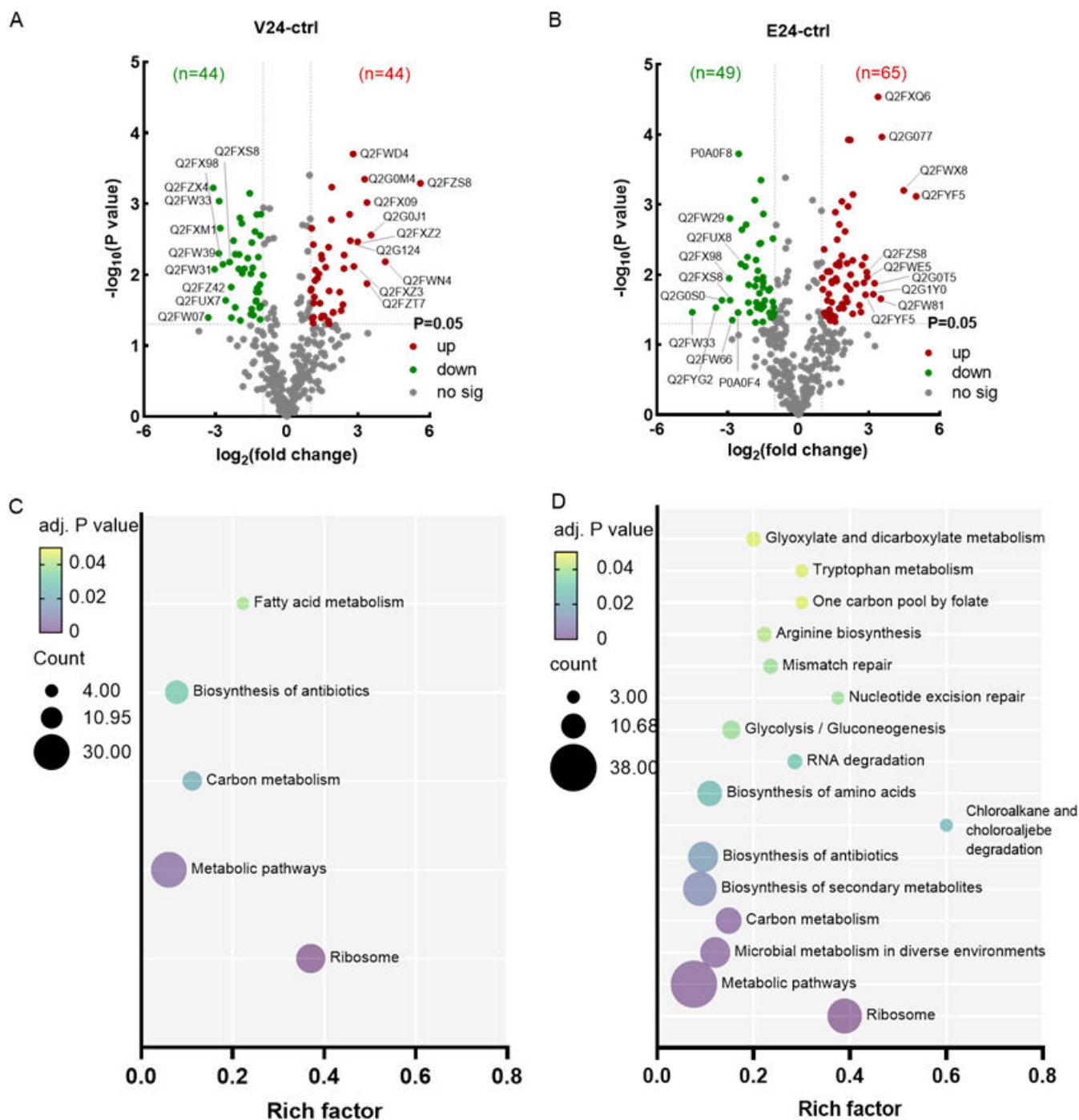


FIG 2 Comparative analysis between persistent populations and control cells. Volcano plots showing differentially expressed proteins ($P < 0.05$) in the vancomycin-triggered persistent populations V-24h (A) and the enrofloxacin triggered persistent population E-24h (B) compared with untreated control samples. Proteins with higher or lower expression level were labeled as red or green, respectively. Uniprot ID of top 10 predominant proteins was labeled in each group. Proteins without significant differences in expression are shown as gray dots. KEGG pathway enrichment analysis was conducted with all differentially expressed proteins in V-24h (C) and E-24h (D). The enrichment factor is calculated as "identified protein numbers annotated in this pathway term"/"all protein numbers annotated in this pathway term."

during the formation and maintenance of persisters under both vancomycin and enrofloxacin treatment. Moreover, DNA repair is strongly associated with persistence under enrofloxacin exposure. To gain further insights into these pathways, we analyzed their dynamics and possible roles in the generation and maintenance of persisters.

TABLE 1 Top 10 increased proteins (non-shaded) and decreased proteins (shaded) in V-24h and E-24h samples compared with control samples

V-24h vs ctrl			E-24h vs ctrl		
Uniprot ID	Protein name	Log ₂ (FC)	Uniprot ID	Protein name	Log ₂ (FC)
Q2FZS8	Chaperone protein ClpB	5.61	Q2FZS8	Chaperone protein ClpB	5.01
Q2FWN4	Chaperonin GroEL	4.14	Q2G046	UvrABC system protein A	4.48
Q2G0J1	Coproheme decarboxylase	3.53	Q2FWE5	SHMT	3.55
Q2FZT7	Signal peptidase I	3.37	Q2G1Y0	Polydeoxyribonucleotide synthase [NAD(+)]	3.50
Q2F × 09	Response regulator protein VraR	3.36	Q2G0T5	DNA polymerase III subunit	3.38
Q2G0M4	BCAT	3.27	Q2FXQ6	Trigger factor	3.24
Q2FXZ2	Chaperone protein DnaK	2.98	Q2FW81	Uridyltransferase	3.18
Q2FXZ3	Chaperone protein DnaJ	2.82	Q2G077	Ribonucleoside-diphosphate reductase	2.91
Q2FWD4	MurA	2.78	Q2FYF5	(d)CMP kinase	2.85
Q2G124	Probable acetyl-CoA acyltransferase	2.66	Q2FZ78	Pseudouridine synthase	2.83
Q2FW07	50S ribosomal protein L4	-3.30	Q2FW33	50S ribosomal protein L17	-4.51
Q2FZX4	Lipoyl synthase	-3.10	Q2FYG2	DNA-binding protein HU	-3.50
Q2FW31	30S ribosomal protein S11	-3.04	Q2G0S0	General stress protein CTC	-3.25
Q2FW39	30S ribosomal protein S9	-2.86	Q2F × 98	HTH cro/C1-type domain-containing protein	-2.94
Q2FW33	50S ribosomal protein L17	-2.85	Q2FW29	50S ribosomal protein L36	-2.91
Q2FXM1	Usp domain-containing protein	-2.80	Q2FXS8	50S ribosomal protein L21	-2.90
Q2F × 98	HTH cro/C1-type domain-containing protein	-2.69	Q2FW66	Alkaline shock protein 23	-2.81
Q2FUX7	Arginine deiminase	-2.57	P0A0F4	50S ribosomal protein L11	-2.57
Q2FXS8	50S ribosomal protein L21	-2.40	P0A0F8	50S ribosomal protein L15	-2.53
Q2FZ42	50S ribosomal protein L19	-2.34	Q2FUX8	Ornithine carbamoyltransferase	-2.45

Central carbon metabolism

Central carbon metabolism is essential in both energy production and the provision of precursors for other essential cellular processes. Interesting pathways with expression level of relevant enzymes in V-24h and E24h were visualized in Fig. 3A. The dynamics of stated enzymes are visualized in a heatmap (Fig. 3B) shown in red and green for higher and lower expression compared with untreated samples, respectively. In general, in V-24h and E-24h, glycolysis was differently regulated. Meanwhile, the expression of most citrate cycle (TCA cycle) enzymes was reduced but pyruvate oxidation, pentose phosphate pathway (PPP), and one-carbon metabolism (OCM) were induced under both stress conditions. The details are discussed in the following paragraphs.

Glycolysis is the initial pathway of utilizing glucose, the primary carbon source in culture medium. Proteomics data show that glycolysis-involved proteins were overexpressed since the first hour of vancomycin treatment but were gradually repressed in cells exposed to enrofloxacin, indicating a difference in carbon source consumption. To investigate this, we conducted high-performance liquid chromatography (HPLC) analysis to monitor glucose consumption (Fig. 3C) and acetate production (Fig. 3D) during antimicrobial exposure. Together with the biphasic kill curves (referenced from Fig. 1A) in each diagram, we found that, clearly, during the initial 4 hours where most of the killing occurred, surviving cells were still able to quickly consume glucose and secrete acetate in both conditions with similar activity. After this time point, glucose consumption ceased in enrofloxacin persists, and less amount of acetate was generated. Meanwhile, however, vancomycin persists still had active, though relatively slower, carbon metabolic reactions.

Glycolysis is also an integral precursor provider in *S. aureus* to generate macromolecules such as amino acids, lipids, and cell wall precursors (20). For example, enzyme activities in V-24h lead to possible accumulation of fructose-6-phosphate, a glycolytic intermediate for cell wall biosynthesis (21). Pyruvate is another important precursor generated from glycolysis to form acetate, oxaloacetate and acetyl-CoA. Acetyl-CoA carboxylase carboxyltransferase (Q2FXM7) was elevated in both stress conditions to initiate type II fatty acid biosynthesis.

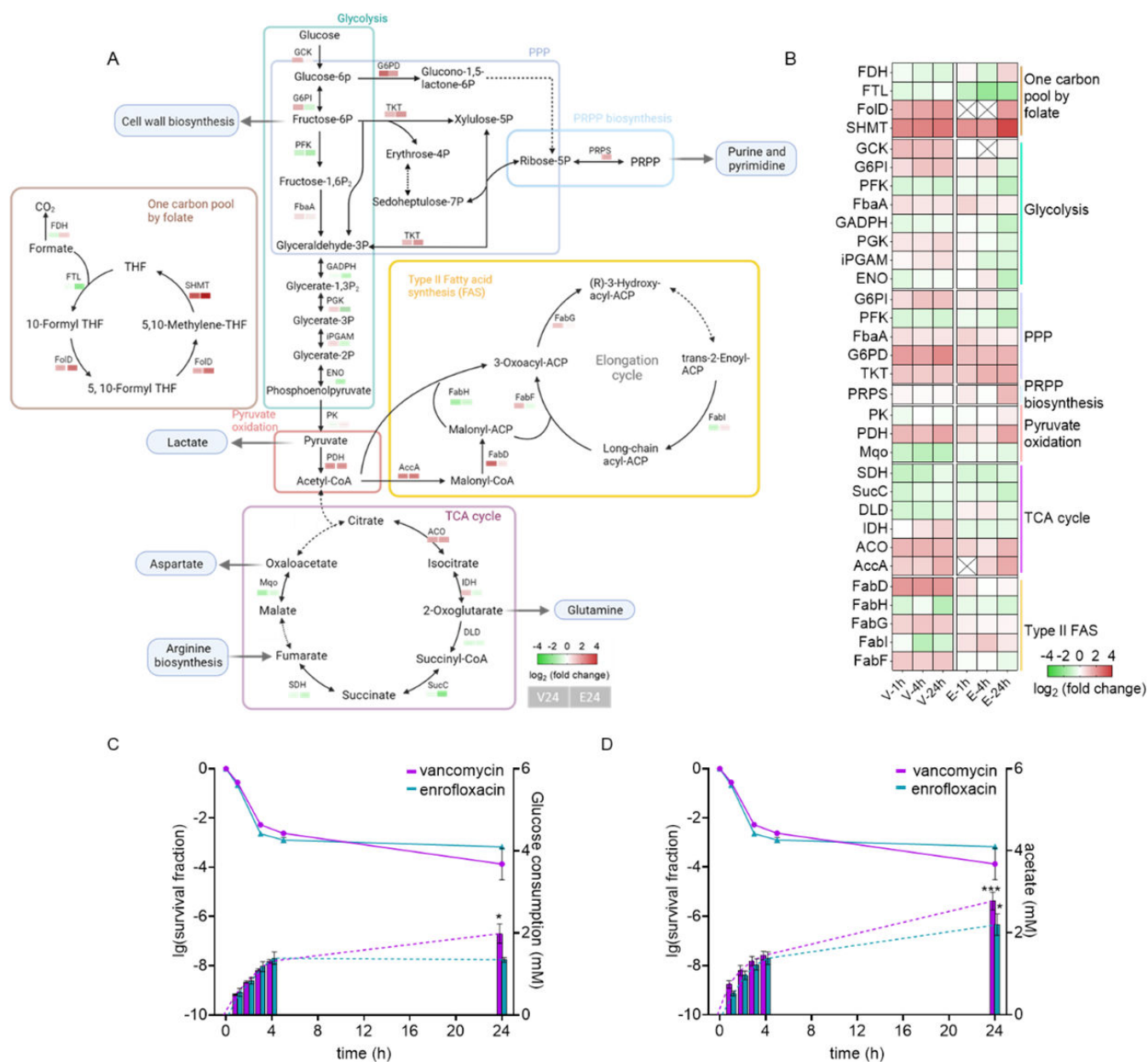


FIG 3 Alteration in central carbon metabolism during vancomycin and enrofloxacin exposure. (A) Schematic map showing the fold change of relevant enzymes (labeled with UniProt protein ID) in both V-24h and E-24h. (B) The dynamics of involved proteins during the biphasic kill curve. In both panels A and B, green filled squares mean lower expression level, while red ones are increased compared with the control group. A cross means not detected. To detect the carbon metabolic activity during antimicrobial exposure, HPLC was conducted to measure the glucose consumption (C) and acetate excretion (D). Biphasic kill curves from Fig. 1A are shown together with HPLC dynamics in each diagram. Six biological replicates were used and the data are shown as mean \pm SD. Unpaired *t*-test was used to detect the difference between 4- and 24-hour treated samples in each treatment group. **P* < 0.05, ****P* < 0.001. HPLC, high-performance liquid chromatography; PPP, pentose phosphate pathway; PRPP, phosphoribosyl pyrophosphate; THF, tetrahydrofolate.

Under laboratory conditions and exponential growth, TCA cycle enzymes are often repressed or dispensable for viability (22). Here in the growth-arrested persistent populations, most enzymes of the TCA cycle were, as expected, repressed. Still, several enriched enzymes can be seen in the treated groups, which might be due to their role in the provision of precursors. For instance, vancomycin triggered the expression of CitZ, the initial enzyme of the TCA cycle, causing possible 2-oxoglutarate (2-OG) accumulation. Consistent with the literature (23), this vancomycin-triggered 2-OG buildup can

contribute to the steady generation of glutamine, which eventually benefits cell wall biosynthesis. Vancomycin also uniquely induced the expression of FumC that was also overexpressed in persistent *S. aureus in vivo*, leading to fumarate level decrease and, by that, glycolysis activation (24).

PPP was elevated in both V-24h and E-24h, which is able to replenish NADPH that was consumed by the indicated pathways such as branched-chain amino acids biosynthesis, fatty acid biosynthesis, glutamine biosynthesis, as well as one carbon metabolism. Additionally, PPP also links to phosphoribosyl pyrophosphate (PRPP) biosynthesis, which is the rate-limiting step in purine and pyrimidine biosynthesis (25). In E-24h, enhanced synthesis of PRPP could aid in *de novo* nucleotide synthesis, which is strongly linked to DNA replication, survival, and antibiotic persistence in *S. aureus* (26, 27). Last but not least, folate-based OCM was induced in both stress conditions, and tetrahydrofolate (THF) accumulation was expected based on the enzyme expression pattern. THF was found to directly participate in crucial metabolic activities including the synthesis of nucleotides, purines, and amino acids (28). Besides, in *E. coli*, the overexpression of 5-formyltetrahydrofolate cyclo-ligase (Q2FZJ6 in *S. aureus*) promotes persister formation upon ampicillin and ofloxacin exposure (29).

In summary, this described metabolic rewiring suggests that persisters, despite being growth arrested, alter their metabolic pathways to favor energy needs and the provision of precursors for essential cellular processes in response to antimicrobial treatment. Additionally, this adaptation may also allow persisters to conserve energy and resources until conditions become favorable for regrowth.

Chaperones

Chaperone proteins play a critical role in facilitating the proper folding of proteins in all living cells (30). Their importance in persister formation and resuscitation was proven in several bacterial species including *S. aureus* (31–34). In our study, we identified 10 chaperone proteins that were overexpressed in almost all treated samples (Fig. 4A), with ClpB being the top overexpressed protein in both vancomycin- and enrofloxacin-persistent populations (see Table 1). The ClpB-DnaK system has been shown to be vital for persister survival and resuscitation due to its ability to clear protein aggregates (33). We also found increased ClpP and ClpX that associate with ATPase ClpC to form ClpPC and ClpPX proteases and facilitate persister formation via the degradation of antitoxins (35). ClpX is also essential for cell viability in suboptimal environments including the presence of oxidative stress (36, 37), which may explain the steady increase of ClpX under enrofloxacin exposure. In addition to the Clp proteases, other chaperones such as DnaK, DnaJ, and GroEL were also overexpressed and are crucial in bacterial protein folding upon exposure to antibiotic stress (38, 39). The deletion of DnaK leads to perturbed stress response and decreased persistence (40). In contrast, ClpL, *cis/trans* isomerase trigger factor (TF), and PrsA are with little known function or evidence in terms of antibiotic persistence. However, TF was reported to promote biofilm formation and interact with ClpB (41), while PrsA was also involved in VraSR-regulated cell wall stress response (42).

Additionally, compared with untreated control samples, the increase in chaperone levels was seen within the first hour of vancomycin and enrofloxacin exposure, indicating the essential function of chaperones under the given stress conditions. Besides, vancomycin stimulated slightly more chaperones than enrofloxacin, which suggests a difference between these two persistent populations. These assumptions were supported by isolating and visualizing intracellular insoluble proteins (Fig. S1) during the biphasic kill curve, where aggregated proteins were observed within the first hour of incubation in all treated samples. Interestingly, the aggregation levels within vancomycin-treated samples increased along the incubation, while the enrofloxacin-treated samples displayed a decrease in protein aggregation over time.

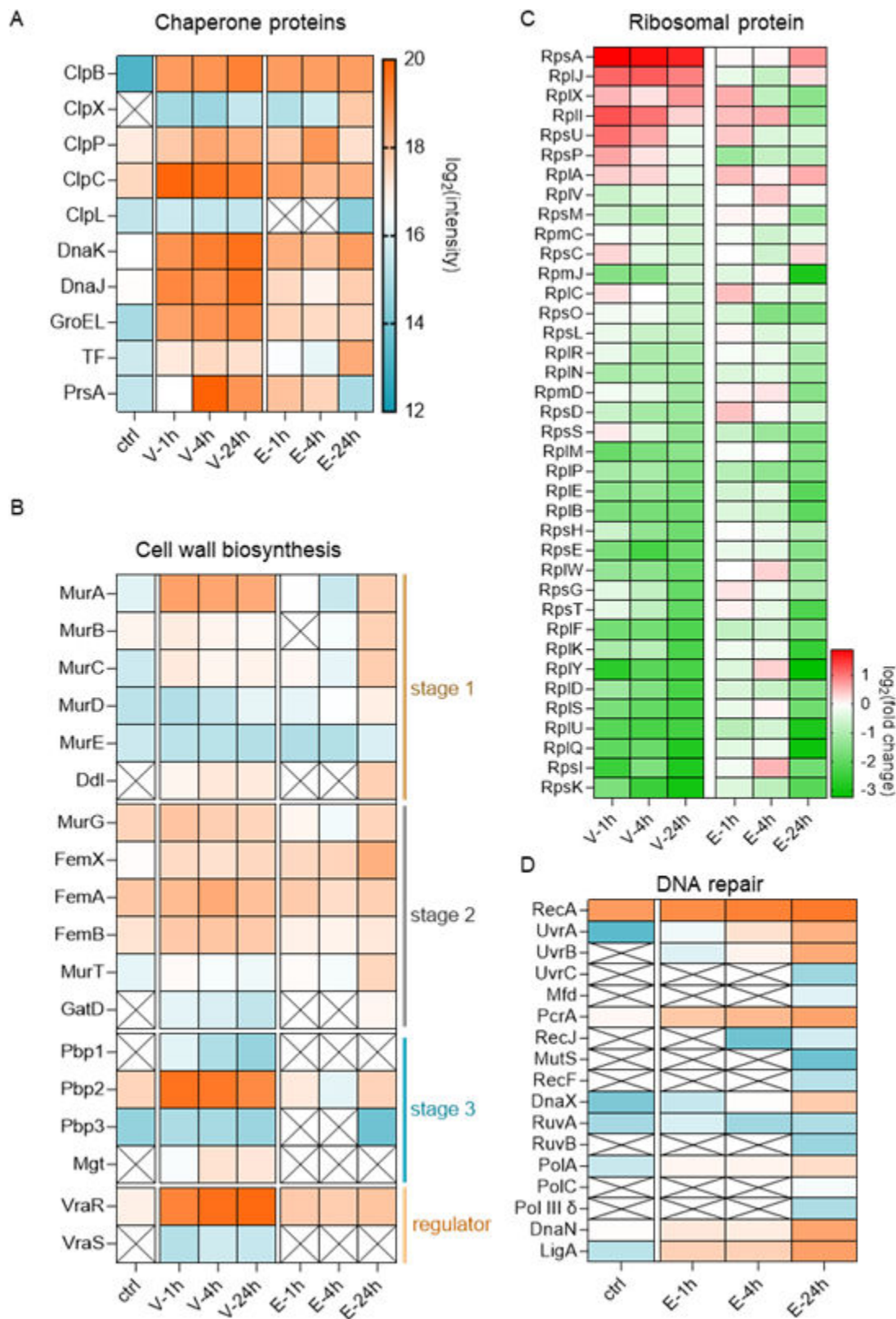


FIG 4 Dynamics of the abundance of (A) chaperone proteins, (B) cell wall biosynthesis-related proteins, (C) ribosomal proteins, and (D) DNA repair-related proteins. For panels A, B, and D, the expression levels of each protein are shown in color ranging from blue (low expression) to orange (high expression). A cross means not detected. In panel C, the expression levels of ribosomal proteins are shown as \log_2 (fold change) compared with control, in which green represents decreased proteins and red shows increased proteins.

Cell wall biosynthesis

In total, 19 proteins involved in cell wall biosynthesis were identified (Fig. 4B). Particularly, 17 proteins participated in the three stages of biosynthesis of peptidoglycan (PG) (43, 44). The first stage involved the synthesis of the peptidoglycan precursor uridine diphosphate (UDP)-MurNAc-pentapeptide in the cytoplasm, with enzymes such as MurA-E and Ddl being detected in our experiments. In stage 2, we identified MurG, the FemXAB family, and the MurT/GatD enzyme-complex, which stimulate the assembly and membrane translocation of lipid II. In stage 3, where the cross-linking of peptidoglycan occurs, enzymes Pbp1-3 and Mgt were detected. Additionally, we found the presence of the VraS/VraR two-component regulatory system. Upon cell wall stress, VraR regulates more than 40 proteins including Pbp2 and Mgt (23), with VraS functioning as a rapid stress sensor (45).

While KEGG enrichment analysis suggests that cell wall synthesis contributes to persistence under both vancomycin and enrofloxacin exposure, different dominant mechanisms in each group are shown. During vancomycin exposure, the highly induced proteins (>5-fold compared to control cells) participate in all three stages of PG synthesis and the VraSR regulon, supporting the idea that a general enhanced cell wall biosynthesis is induced to combat vancomycin, rather than just the synthesis stage three, where vancomycin targets. In addition, all changes happened within the first hour of vancomycin exposure, implying an instantaneously enhanced induction of a stress protective mechanism against this cell wall-targeting antibiotic. In comparison, the various proteins in enrofloxacin-triggered persistent population were mostly featured in stage 1 of PG biosynthesis and displayed a relatively mild but consistent increase during the treatment. Here, the lack of induction of the VraS regulon might indicate that the induced peptidoglycan biosynthesis by enrofloxacin is not due to cell wall stress.

Ribosomal proteins

A ribosome-dependent translation block is considered as one of the hallmarks of persistence (46). In total, we identified 38 ribosomal proteins in both V-24h and E-24h. The binary logarithm of fold change compared with control was calculated and shown in the heatmap (Fig. 4C). In general, the amounts of ribosomal proteins were expectedly reduced. Interestingly, most proteins with reduced abundance, especially in enrofloxacin-treated samples, were gradually decreased during the biphasic kill curve instead of quickly reaching their final levels. Besides, four slightly higher expressed ribosomal proteins can be seen, respectively, in V-24h (ribosome initiation protein RpsA, RplJ contributing to the binding of elongation factor, assembly initiator protein RplX, and RplI that influences tRNA stability) and in E-24h (RpsA, RplJ, RplA that involved in releasing tRNAs, and RpsC which is essential for mRNA entrance) (47, 48). Overall, these alterations not only benefit persister formation by repressing unnecessary translation but also allow cells to synthesize stress response-related proteins and to maintain the potential for resuscitation.

DNA repair

We identified 21 proteins related to DNA repair in E-24h (Fig. 4D), including SOS response inducer RecA; nucleotide excision repair-related proteins UvrABC, Mfd, and PcrA; mismatch repair involved RecJ and MurS, homologous recombinant proteins RecF, DnaX, RuvA and RuvB, DNA replication-related proteins Pol I (PolA), Pol III subunits PolC, Pol III δ , and DnaN, as well as DNA ligase LigA to join breaks and fill the gap generated during DNA repair and replication (49–52). Of these, SOS response is regarded as a key response inducing persister formation via repair of DNA damage, altering DNA expression and sometimes modulating the toxin-antitoxin system (53). Upon DNA damage, the positive regulator RecA recognizes the damage and likely binds to single-stranded DNA to initiate the SOS response (54). UvrABC, RuvAB, and RecF are also associated with the SOS response and are regulated by RecA. All 21 detected proteins

either steadily increased during the treatment under enrofloxacin or were detected only after a few hours of stress incubation, showing their significance in both persister formation and maintenance. The different dynamics and appearance time of enzymes suggest their putative specific function in certain stages of persister formation.

Comparison between persistent populations generated from different stress conditions

The stated comparison between treated and untreated samples suggests that the detailed protein compositions for vancomycin or enrofloxacin persistent populations are distinct. Therefore, we comparatively analyzed the proteome and metabolomic features of V-24h and E-24h.

Firstly, volcano plots (Fig. 5A) show that, in total, 107 proteins out of 483 shared proteins are differentially expressed ($P < 0.05$), among which 48 proteins were overexpressed in V-24h and 59 proteins in E-24h. Together with distinctively expressed proteins shown in Fig. 2, a total of 90 proteins in V-24h and 138 proteins in E-24h were used for KEGG enrichment analysis (Fig. 5B). We matched eight pathways in V-24h that are associated with the biosynthesis of amino acids, microbial metabolism in diverse environments, biosynthesis of secondary metabolites, and carbon metabolism. Proteins involved in biosynthesis of amino acids are responsible for the production of branched-chain amino acids, threonine, arginine, glutamine, proline, and tryptophan. In E-24h, only six pathways were enriched: mismatch repair, nucleotide excision repair, homologous recombination, DNA replication, pyrimidine metabolism, and metabolic pathways. Again, this result demonstrates that DNA repair-related pathways are main contributors to enrofloxacin-induced persisters.

Then, metabolomics was performed with 24-hour-treated persistent populations. Principal component analysis (PCA, Fig. 5C) shows qualified replicates and distinct profile in V-24h and E-24h samples. KEGG analysis resulted in eight significantly enriched pathways (adjusted P value < 0.05): metabolic pathways, pentose phosphate pathway, glycolysis/gluconeogenesis, methane metabolism, vitamin B6 metabolism, purine metabolism, pyrimidine metabolism, and terpenoid backbone biosynthesis. The average intensity of each involved metabolite was normalized with V-24h and shown as \log_2 (fold change) (Fig. 5D), where positive values present higher intensity in V-24 (in blue) and negative values show more accumulation in E-24h (in red). Consistent with proteomics results that glycolytic enzymes were induced by vancomycin but repressed by enrofloxacin, vancomycin-induced persisters had relatively less accumulation of D-fructose-1,6-bisphosphate, glyceraldehyde-3-phosphate, and D-glycerate-2-phosphate. In purine metabolism, higher amounts of GMP, dGDP, and GDP in V-24h were detected. This also supports the hypothesis that more (P)ppGpp was generated, and by that, the stringent response was activated to combat vancomycin exposure. In E-24h, the annotated metabolites in pyrimidine metabolism accumulated, which might favor DNA synthesis to respond against enrofloxacin exposure. As a common enriched pathway, the interaction network of pyrimidine-related proteins and metabolites was depicted (Fig. 5E). Positive Pearson correlations were observed between the changes in the identified metabolites and proteins, indicating that these changes were likely interrelated.

Differences in persistence mechanisms suggest new insights in how to eliminate persisters

Above, we compared the molecular profiles of persistent populations induced by vancomycin or enrofloxacin, revealing both similarities and differences. As depicted in Fig. 6A, both vancomycin and enrofloxacin triggered persisters with more chaperones, elevated cell wall biosynthesis, less ribosomes and altered carbon metabolism. Meanwhile, vancomycin also stimulated the stringent response and potentially altered membrane composition by generating more branched-chain amino acids by proteins increased in expression as shown by the proteomics results. For enrofloxacin persisters, DNA repair pathways and ABC transporters were more prominently observed.

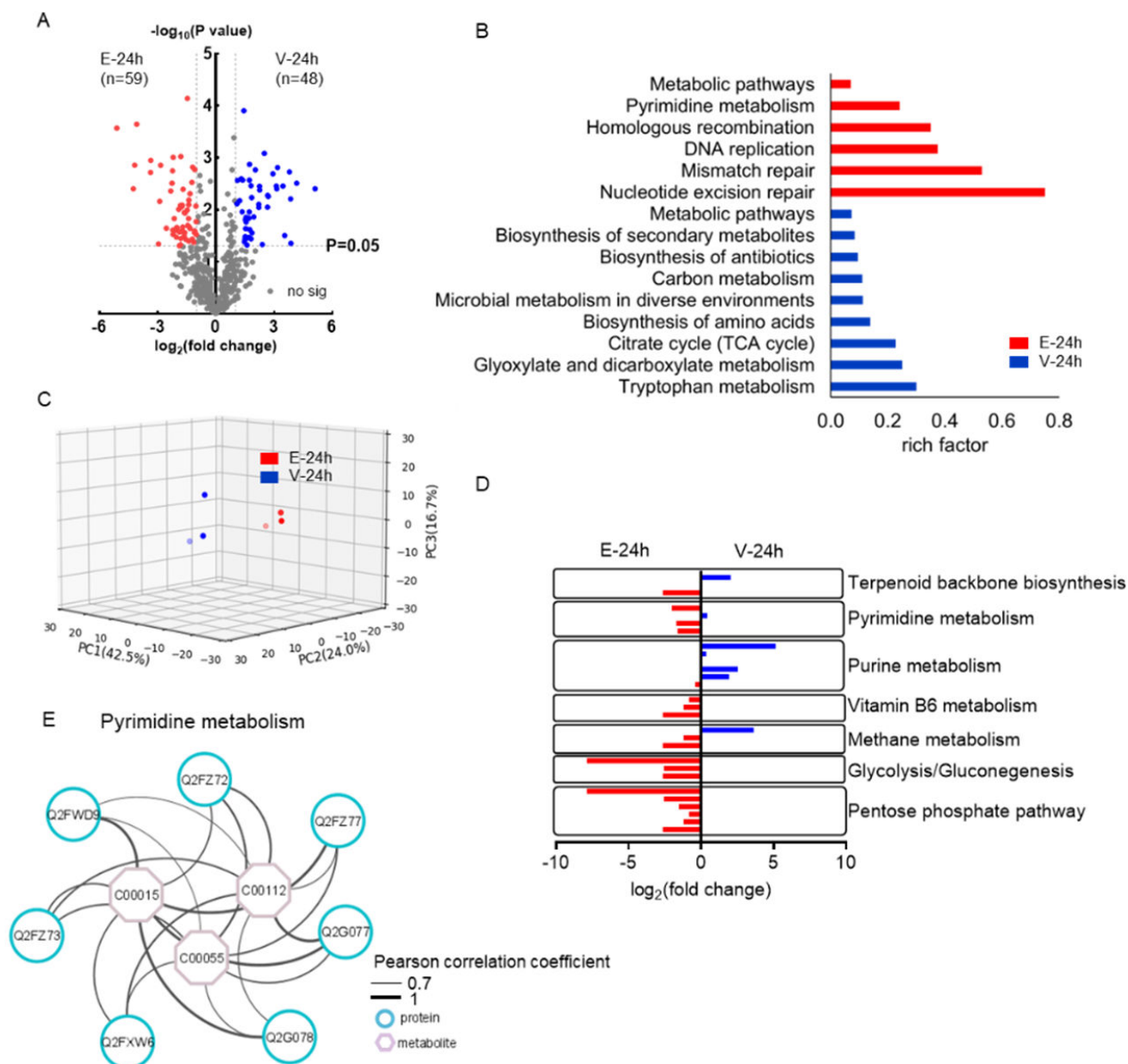


FIG 5 Comparison of proteins and metabolites in persistent populations generated by vancomycin or enrofloxacin exposure. (A) t -Test of shared proteins between V-24h and E-24h ($n = 483$). (B) KEGG enrichment analysis was performed separately for V-24h and E-24h with significantly expressed proteins plus uniquely expressed proteins. Only pathways with adjusted P values of <0.05 were shown. (C) Principal component analysis of 95 identified metabolites present in V-24h (blue) and E-24h (red). The plot displays two distinct clusters indicating good correlation between replicates and clear metabolic profile difference between V-24h and E-24h. (D) KEGG enrichment analysis with 95 metabolites (adjusted P value of <0.05). For comparison between V-24h and E-24h, the average intensity was normalized with V-24h and shown as \log_2 fold change. Each bar represent one enriched metabolite. (E) As a common enriched pathway, the interaction map of proteins and metabolites involved in pyrimidine metabolism was analyzed. Only edges and nodes with Pearson correlation coefficients of ≥ 0.7 are shown. The line thickness represent the correlation value between 0.7 and 1.0. The blue circles represent proteins, and pink octagons are metabolites.

By understanding the mechanisms that underlie persister formation and maintenance, we may gain insights into how to effectively eliminate these cells. We hypothesized that similarities in molecular signaling pathways related to persister growth arrest may lead to cross-tolerance. This was confirmed experimentally as exposure to enrofloxacin of vancomycin surviving cells and *visa versa* failed to kill more cells after the initial persister formation (Fig. 6B). Besides, the differences between persistent populations make combined therapy a potent strategy to avoid high level of persistence. As shown in

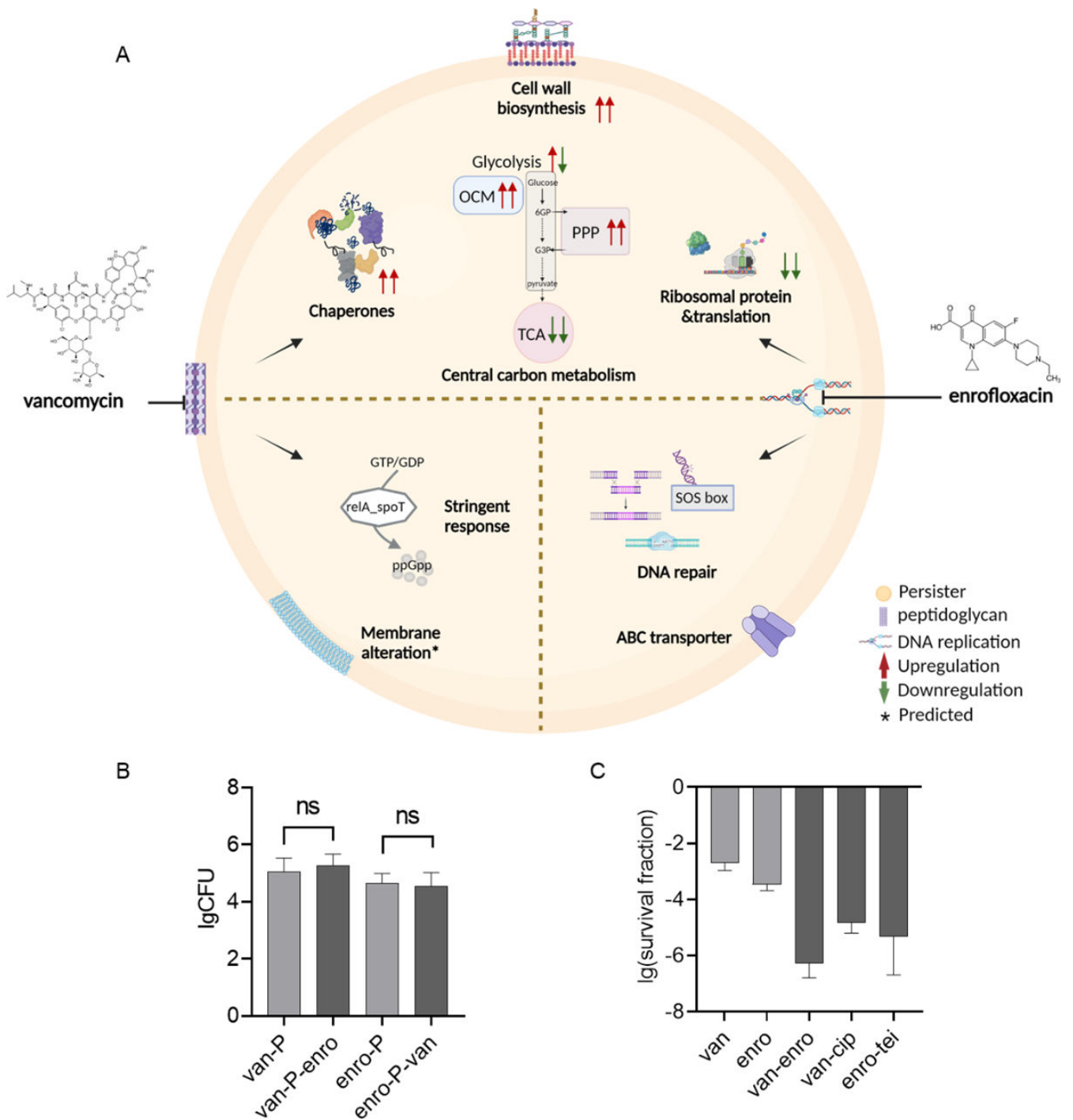


FIG 6 (A) Scheme of the similar and unique mechanisms of persister formation induced by vancomycin and enrofloxacin. For the upper area showing a commonly altered pathway, arrows indicate the upregulation (red) or downregulation (green) of relevant pathways in either vancomycin persisters (left arrow) or enrofloxacin persisters (right arrow). The lower parts indicate unique pathways that are involved in either vancomycin persisters (left) or enrofloxacin persisters (right). (B) Cross-tolerance testing of *S. aureus* persisters reveals that the persistent population generated from a single drug remained unaffected after an additional 2 hours of cross-treatment with another drug. $n = 9$. (C) Treatment with a combination of drugs (50-fold MIC + 50 fold MIC) resulted in more killing than the single treatment (100-fold MIC). The minimum detectable survival fraction was 10^{-8} . At least three biological replicates were used, and the data are shown as mean \pm SD. cip, ciprofloxacin; enro, enrofloxacin; MIC, minimum inhibitory concentration; tei, teicoplanin; van, vancomycin.

Fig. 6C, combining vancomycin and enrofloxacin in one treatment resulted in a significant increase in cell death, over 1,000 times more than each of the single treatments. This suggests that the pathways bacteria used to generate persisters in single treatment were either inefficient or disrupted by the addition of the other drug, e.g., DNA damage caused by enrofloxacin could potentially interfere with relevant gene expression which the bacteria apply to persist under vancomycin pressure. We then also demonstrated a similar synergistic effect for the combination of vancomycin and another fluoroquinolone antibiotic ciprofloxacin, as well as with enrofloxacin combined with cell wall-targeting teicoplanin. This corroborates the potential of combination therapy to effectively reduce persisters rather than relying on sequential use of different antibiotics.

DISCUSSION

In this work, we collected samples during the biphasic kill curve to reveal mechanisms associated with persister formation and maintenance. Only 0.1% of cells of initial cultures become persisters, as shown in the kill curve. However, after 24 hours of antibiotic exposure, most of the sensitive cells were dead and lysed. During sample collection, most debris was then washed away. In the FACS analysis, on average, 75% of the detected cells remaining from the antibiotic-treated cultures were CFDA⁺-propidium iodide (PI)⁻ as and thus persisters. Therefore, it is reasonable to say that proteins and metabolites in V-24h and E-24h mainly came from persistent cells.

Persisters, for decades, had been considered as subpopulations of bacteria without measurable metabolic activity. However, increased research evidenced that while persistent populations are non-dividing, certain metabolic pathways are still active to combat stress and to retain viability waiting for environmental conditions to improve and resuscitation to take place. Our results also demonstrate that persisters are, to a certain level, metabolically active. Even under long-term stress from high levels of bactericidal antibiotics, persisters are still able to consume glucose, synthesize new proteins, and regulate several metabolic pathways. In enrofloxacin-triggered persisters, especially, we identified the unique expression of ABC transporters. This suggests that active extrusion of enrofloxacin may also play a role in generating persistence and likely benefits the cells afterward resuscitation as well. Additionally, metabolic activity levels in two persistent populations induced by different antibiotics are likely different. Straightforwardly, as shown in Fig. 3C, vancomycin persisters are more active in glucose consumption and acetate production than enrofloxacin persisters. This hypothesis can also be inferred from the level of chaperones that aid in preventing protein aggregates and ribosomes. A correlation between protein aggregation level and cell dormancy was proposed (55). Specifically, controlled protein aggregation is suggested to facilitate persister formation by inactivating unnecessary metabolic activities, but excessive aggregation leads to deeper dormancy and even cell death. Thus, the different chaperone expression and aggregated protein levels observed in samples treated with vancomycin and enrofloxacin suggest that greater efforts were needed to sustain a specific level of protein aggregation in vancomycin-treated samples, particularly at V24-h, which could be one of the contributors to stimulate active carbon metabolism. Another indicator is the varying alteration in ribosomal protein expression between two persistent populations. Wood et al. (56) discussed that while repressing ribosomes contribute to persister formation by reducing protein translation to force cells to enter dormancy, a certain intracellular ribosome level is essential for persisters to survive and resuscitate. With proteomics, we found lower expression of ribosomal proteins in both treated populations compared with untreated cells, but V-24h contained higher levels of ribosomal protein than E-24h. Overall, vancomycin persisters exhibit potentially higher metabolic activity than enrofloxacin persisters, which could also cause a difference in resuscitation rate.

One interesting finding is that the vancomycin-triggered alterations mostly happened within 1 hour of antimicrobial incubation, while most changes in enrofloxacin-treated samples appeared only after four hours of exposure. In terms of the modes of action,

vancomycin directly targets the cell wall, while enrofloxacin needs to invade cells before inhibiting DNA synthesis. While this does not necessarily determine the killing efficiency of vancomycin and enrofloxacin, the fast stress responses of bacteria could be due to the instantaneous interaction between vancomycin and the cell wall. It is worth noting that the sampling time point might shape the conclusion in terms of persister formation mechanisms and even the efficacy of persister eradication due to the distinct stress response “reaction time” of certain pathways or specific enzymes. Time-resolved analysis is thus highly advocated.

Furthermore, our omics data provided valuable insights into the biophysical characteristics of persisters that might contribute to persister formation. One notable finding is the modulation of important precursors via central carbon metabolism, which could lead to corresponding phenotype changes in the cell envelope. For example, higher production of branched-chain amino acids helps to maintain membrane fluidity (57). Moreover, perturbed cell wall biosynthesis may lead to thicker cell walls as well as changed cell size. The results also hint to the increased risk of resistance development during resuscitation as persisters contain a higher level of resistance accelerating VraR, Pbp2, and SOS response-related proteins (58–60). Still, further validation studies, e.g., using specific mutants and a pure persister population, are required for more detailed causal mechanistic analysis.

This study, which identifies molecular physiology that adapt *S. aureus* to become persisters when exposed to two types of antibiotics, is highly clinically relevant for preventing antibiotic failure. Noticeably, in this study, two types of antibiotics that triggered similar persister levels led to distinctive proteome and metabolome profiles. In comparison to clinical isolates of *S. aureus* persisters that were triggered by cell wall-targeting flucloxacillin and protein synthesis-inhibiting clindamycin, several opposite changes were observed, including overexpressed ribosomal proteins and repressed DNA repair activity (32). These findings suggest that at the molecular physiological level, persisters exhibit a high degree of stress-specific responses. This implies that the molecular characteristics observed in a population of persisters induced by one stressor may differ or even be opposite to those induced by another stressor. In this case, the efficiency of an antipersister strategy active against persisters induced by one antibiotic will not be guaranteed effective against a persistent population generated by another. Therefore, combinations of antibiotics can be sought to mutually inactivate the mechanisms which the bacteria utilize to generate persisters against either of the antibiotics in single treatment. This way, persister formation may be prevented, allowing proper treatment of patients and eliminating the entire reservoir of the infection. Meanwhile, for generated persisters triggered by one antibiotic, the sequential use of another tested drug did not lead to more killing. In this case, the combination of metabolic-dependent antibiotics could be conducted to eliminate existing persisters (61). Future studies should focus on more detailed mechanistic analyses, preferably in isolated persisters, including the use of mutant strains to advance from the current molecular characterisations and correlations to understanding causative relations.

MATERIALS AND METHODS

Strain cultivation and time-kill kinetics assay

Staphylococcus aureus ATCC 49230 strain (UAMS-1, a highly virulent clinical isolation from a patient with chronic osteomyelitis) was used in this experiment and was incubated at 37°C with shaking at 200 rpm, unless otherwise specified. Overnight culture from a single colony cultured in tryptic soy broth (TSB) was 1:100 inoculated into fresh TSB medium and incubated until early log phase ($OD_{600} = 0.4–0.6$) to avoid population heterogeneity and persisters caused by the lack of nutrition. The culture was then diluted with fresh TSB to $OD_{600} = 0.2$ to ensure a consistent initial concentration. Diluted culture was divided into three Erlenmeyer flasks for three treatment groups. One of the cultures without

antibiotic exposure was used as control. For the other two flasks, antibiotics were added separately to a final concentration of 100-fold minimum inhibitory concentration (MIC) for single treatment or 50-fold MIC for combined treatment. MIC measurement and the quantification of CFU were performed following the previous protocol (62). The MICs of each antibiotic (all purchased from Sigma-Aldrich Chemie NV, the Netherlands) are vancomycin 1 $\mu\text{g}/\text{mL}$, enrofloxacin 0.25 $\mu\text{g}/\text{mL}$, teicoplanin 0.25 $\mu\text{g}/\text{mL}$, and ciprofloxacin 1 $\mu\text{g}/\text{mL}$. The MIC of the surviving population was also measured to make sure no resistant bacteria were selected.

For time-kill kinetics assay, aliquots of 1 mL of culture were removed before and after 1, 3, 5, and 24 hours of antibiotic exposure and washed twice with phosphate-buffered saline (PBS) buffer to remove antibiotics. Surviving cells in each sample were then quantified by quantitative culture of 10-fold serial dilutions with PBS plated on TSB agar plate. After overnight incubation, the number of colonies was quantified, and the surviving fraction of treated samples compared with control was calculated and visualized as kill curve. For cross-tolerance, 100-fold MIC of enrofloxacin or vancomycin was added directly into 24-hour vancomycin or enrofloxacin-treated samples, respectively. Then, 2-hour incubation was performed before quantification. To detect the proportion of persister cells after antibiotic exposure, double staining of 5- (and 6-) -carboxyfluorescein diacetate that labels metabolically active cells and PI that marks dead cells was used. CFDA⁺-PI⁻ cells were considered to be persisters in antibiotic-treated cultures for subsequent flow cytometry analysis essentially according to reference (62) and further detailed for *S. aureus* in bioRxiv reference (15). In more than 30 independent flow cytometry experiments of persisters of *S. aureus* (not all data were shown in Fig. 1B) using the described method, we isolated around 75% of persisters.

Extracellular metabolite measurement

Extracellular medium was filtered by 0.22- μm filters before and during 1-, 2-, 3-, 4- and 24-h antibiotic incubation. The standards for the HPLC measurement of glucose and acetate were prepared with a set of concentration within 0–50 mM. All standards and samples were measured by HPLC (LC-20AT, Prominence, Shimadzu) equipped with Ion exclusion Rezex ROA-Organic Acid H⁺ (8%) column (300 \times 7.8 mM, Phenomenex), along with a guard column (Phenomenex). The injection volume was set to 50 μL using the SIL-20AC autosampler (Shimadzu), and the system operated at a pressure of 50 bar. Aqueous H₂SO₄ (5 mM) was used as mobile phase at a flow rate of 0.5 mL/min at 55°C. The UV detection was performed at $\lambda = 210$ nm using the SPD-20A UV/VIS detector, and a refractive index detector was also utilized (RID 20A, Shimadzu).

Sample collection

At the selected time point, the OD₆₀₀ value of each culture was measured. Subsequently, 15 OD units of cells (i.e., the equivalent of 15 mL of a suspension of OD 1) of vancomycin- or enrofloxacin-treated groups was collected during incubation to isolate protein and metabolites. For proteins, samples were collected before and after 1-, 4-, and 24-hour antibiotic exposure. Metabolites from final 24 hour-treated samples were also extracted for metabolomics. The isolation protocol is modified from reference (63). Specifically, after filtration and washing twice with ice-cold 0.6% NaCl solution, filter paper was quickly removed into a 50-mL Falcon tube containing 3-mL ice-cold 60% ethanol as extraction solution. After vigorously vortexing for about 10 seconds, the tube was dropped into liquid nitrogen to quench the metabolism. Samples were stored in -80°C until all triplicate treatment groups were collected and ready for protein and metabolite isolation.

Frozen samples were thawed on ice and mixed by vortexing for 10 seconds to detach the cells from the filter. Afterward, 1 mL of the resulting cell suspension was transferred into a 2-mL homogenizer tube containing 0.5-mL 0.5-mM glass beads, and each sample was aliquoted into three tubes. Cells were then disrupted by Bead Ruptor Elite homogenizer (OMNI International, Georgia, USA). During the beads beating, the ambient

temperature was kept at around 0°C. Next, cell suspensions from the same sample were transferred to a 15 mL tube. The glass beads were washed twice with ice-cold ethanol, and the washing solution was also transferred to the same tube. To separate metabolites and proteins, tubes were centrifuged for 5 min at 10,000 × *g*. Four-milliliter supernatant containing metabolites was transferred and dried by a nitrogen stream. Non-polar and polar metabolites were suspended by isopropanol:acetonitrile:water = 4:3:1 and acetonitrile:water = 1:1, respectively. The rest of the supernatant and pellet with proteins were dried in a centrifugal vacuum evaporator and resuspended with 1% sodium dodecyl sulfate (SDS; Duchefa Biochemie B.V. Haarlem, the Netherlands) in 100-mM ammonium bicarbonate (Sigma-Aldrich Chemie NV).

LC-MS sample preparation and analysis

Metabolomics

The dry apolar metabolites obtained by extractions by monophasic methods were reconstituted in 200- μ L water; the dry polar metabolites were in 200- μ L acetonitrile (ACN):water (1:1). Ten microliters was injected for non-targeted metabolomics onto a CSH-C18 column (100 mM × 2.1 mM, 1.7- μ m particle size; Waters, Massachusetts, USA) for apolar metabolite analysis or an ethylene bridged hybrid (BEH)-amide column (100 mM × 2.1 mM, 1.7- μ m particle size; Waters) for a-polar metabolites by an Ultimate 3000 UHPLC system (Thermo Scientific, Dreieich, Germany). Using a binary solvent system [A: 0.1% formic acid (FA) in water, B: 0.1% FA in ACN], we separated metabolites on the CSH-C18 column by applying a linear gradient from 1% to 99% B in 18 min at a flow rate of 0.4 mL/min, while polar metabolites were separated on the BEH-amide column by applying a linear gradient from 99% B to 40% B in 6 min and then to 4% B in 2 min at a flow rate of 0.4 mL/min. Eluting analytes were electrosprayed into a hybrid trapped ion-mobility-spectroscopy quadrupole time of flight mass spectrometer (TIMS-TOF Pro; Bruker, Bremen Germany), using a capillary voltage of 4,500 V in positive mode and 3,500 V in negative mode, with source settings as follows: end plate offset, 500 V; dry temperature, 250°C; dry gas, 8 L/min; and nebulizer set at 3 bar, both using nitrogen gas. Mass spectra were recorded using a data-dependent acquisition approach in the range from *m/z* of 20–1300 for polar and 100–1,350 for the apolar metabolites in positive and negative ion modes using nitrogen as collision gas. Auto tandem mass spectrometry (MS/MS) settings were as follows: quadrupole ion energy, 5 eV; quadrupole low mass, 60 *m/z*; and collision energy 7 eV. Active exclusion was enabled for 0.2 min, reconsidering precursors if the current:previous intensity ratio was >2.

Proteomics

The pellets obtained above were dissolved in 300- μ L 1% SDS in 100-mM ABC and vortexed thoroughly. The bicinchoninic acid (BCA) assay was used to determine the concentration of protein according to the manual; 10 and 30 mM of tris-(2-carboxyethyl)phosphine (TCEP) and chloroacetic acid (CAA) were added, respectively; and the mix was incubated for 0.5 hours at room temperature. Samples were processed using the SP3 protein cleanup (60); trypsin (protease:protein, 1:50, wt/wt) was added; and protein was digested at 37°C overnight. The supernatant was acidified with FA (1% final concentration and a pH ~2), and while on a magnetic stand to trap magnetic beads, the supernatant was moved to a clean tube. For liquid chromatography-mass spectrometry (LC-MS) analysis, ~200 ng (measured by a NanoDrop at a wavelength of 215 nm) of the peptide was injected by an Ultimate 3000 RSLCnano UHPLC system (Thermo Scientific, Germering, Germany).

Following injection, the peptides were loaded onto a 75 μ m × 250 mM analytical column (C18, 1.6- μ m particle size; Aurora Ionopticks, Australia), kept at 50°C and a flow rate of 400 nL/min at 3% solvent B for 1 min (solvent A: 0.1% FA, solvent B: 0.1% FA in ACN). Subsequently, a stepwise gradient of 2% solvent B at 5 min, followed by 17% solvent B at 24 min, 25% solvent B at 29 min, 34% solvent B at 42 min, and 99%

solvent B at 33 min was held until 40 min, returning to initial conditions at 40.1 min and equilibrating until 58 min. Eluting peptides were sprayed by the emitter coupled to the column into a captive spray source (Bruker) which was coupled to a TIMS-TOF Pro mass spectrometer. The TIMS-TOF was operated in PASEF mode of acquisition for standard proteomics. In PASEF mode, the quad isolation width was 2 Th at 700 m/z and 3 Th at 800 m/z , and the values for collision energy were set from 20 to 59 eV over the TIMS scan range. Precursor ions in an m/z range between 100 and 1,700 with a TIMS range of 0.6 and 1.6 V-s/cm² were selected for fragmentation. Ten PASEF MS/MS scans were triggered with a total cycle time of 1.16 seconds, with target intensity of 2e4 and intensity threshold of 2.5e3 and a charge state range of 0–5. Active exclusion was enabled for 0.4 min, reconsidering precursors if the current:previous intensity ratio was >4.

Data analysis

The metabolite mass spectrometry raw files were submitted to MetaboScape (version 5.0; Bruker Daltonics, Germany), which was used to perform data deconvolution, peak-picking, and alignment of m/z features using the TReX 3D peak extraction and alignment algorithm (EIC correlation set at 0.8). All spectra were recalibrated on an internal lockmass segment (NaFormate clusters), and peaks were extracted with a minimum peak length of seven spectra (eight for recursive extraction) and an intensity threshold of 500 counts for peak detection. In negative mode ion deconvolution setting, [M-H]⁻ was set for primary ion; seed ions were [M+Cl]⁻; and common ions were [M-H-H₂O]⁻ and [M+COOH]⁻. For positive mode, the primary ion was [M+H]⁺; seed ions were [M+Na]⁺, [M+K]⁺, [M+NH₄]⁺, and [M-H-H₂O]⁺ were common ions. Features were annotated using SMARTFORMULA (narrow threshold, 3.0 mDa, mSigma: 15; wide threshold, 5.0 mDa, mSigma: 30) to calculate a molecular formula. Spectral libraries including Bruker MetaboBASE (version 3.0), Bruker HDBM (version 2.0), MetaboBASE (version 2.0) *in silico*, MSDIAL LipidDBs, MoNA VF NPL QTOF, and GNPS export were used for feature annotation (narrow threshold, 2.0 mDa, mSigma: 10, msms score 900; wide threshold, 5.0 mDa, mSigma: 20, msms score 800). An annotated feature was considered to be of high confidence if more than two green boxes were present in the annotation quality column of the program and low confidence if less than two green boxes were present.

After searching and peak-picking, positive and negative profiles were combined for further analysis. Metabolomic data analysis was carried out by using MetaboAnalyst (version 5.0, <https://www.metaboanalyst.ca/MetaboAnalyst/home.xhtml>). At first, the data showing a poor variation were filtered on interquartile range, and then features were normalized by median normalization, scaled by autoscaling and transformed to a logarithmic scale (base of 2).

Generated mass spectra for pellets were analyzed with Maxquant (version 1.6.14) for feature detection and protein identification. TIMS-DDA was set in type of group specific, and other parameters were set as the default. Search included variable modifications of methionine oxidation, and a fixed modification of cysteine carbamidomethyl and the proteolytic enzyme was trypsin with a maximum of two missed cleavage. An *S. aureus* database (version 2019, downloaded from Uniprot) was used for database searches. To improve mass accuracy of matching precursors, the “match between runs” option was applied within a match window time of 0.2 min and a match ion mobility window of 0.05. Proteins of label-free quantification calculated for each pellet represented normalized peptide intensities correlating with protein abundances. Finally, all the quantification and annotation information were summed in in the output proteinGroup.txt.

Proteins and metabolites that were found in at least two replicates were considered to be reproducibly detected and used for analysis. Then data were analyzed by Perseus (64) for log₂ transform, Pearson correlation coefficient analysis, hierarchical cluster analysis, PCA assay, Z-score normalization, and statistical analysis. Significantly expressed proteins are those with |log₂(fold change)| of >1 and *P* value of <0.05. The proteomic pathway

analysis was done with KOBAS (65), and metabolic pathway enrichment was conducted on the website Metabolites Biological Role (version 2.0) (66); only pathways with adjusted *P* values of < 0.05 were considered to be significant.

ACKNOWLEDGMENTS

We acknowledge Gonzalo Congrains Sotomayor for his expert technical assistance in flow cytometry experiments. S.L. acknowledges the China Scholarship Council for her PhD scholarship.

This research was supported by a Chinese Scholarship Council grant (201904910554) awarded to S.L.

Conceptualization: S.B., S.A.J.Z., and S.L.; performance of experiments and analysis of data: S.L., Y.H., S.J., P.L., and G.K.; writing—original draft preparation: S.L.; writing—review and editing: G.K., S.B., and S.A.J.Z. All authors read and agreed to the published version of the manuscript.

AUTHOR AFFILIATIONS

¹Department of Molecular Biology and Microbial Food Safety, University of Amsterdam, Swammerdam Institute for Life Sciences, Amsterdam, the Netherlands

²Laboratory for Mass Spectrometry of Biomolecules, University of Amsterdam, Swammerdam Institute for Life Sciences, Amsterdam, the Netherlands

³Department of Medical Microbiology and Infection Prevention, Amsterdam institute for Infection and Immunity, Amsterdam UMC, University of Amsterdam, Amsterdam, the Netherlands

AUTHOR ORCID*s*

Shiqi Liu  <http://orcid.org/0009-0003-8930-5184>

Stanley Brul  <http://orcid.org/0000-0001-5706-8768>

FUNDING

Funder	Grant(s)	Author(s)
China Scholarship Council (CSC)	201904910554	Shiqi Liu

AUTHOR CONTRIBUTIONS

Shiqi Liu, Conceptualization, Data curation, Formal analysis, Funding acquisition, Writing – original draft, Writing – review and editing | Yixuan Huang, Conceptualization, Data curation, Formal analysis, Funding acquisition, Writing – original draft | Sean Jensen, Data curation, Formal analysis, Investigation | Paul Laman, Formal analysis, Investigation | Gertjan Kramer, Data curation, Formal analysis, Investigation, Writing – review and editing | Sebastian A. J. Zaat, Conceptualization, Data curation, Formal analysis, Writing – review and editing | Stanley Brul, Conceptualization, Data curation, Formal analysis, Funding acquisition, Writing – review and editing

DATA AVAILABILITY

All mass spectral data related to this publication have been deposited in the MassIVE repository (<https://massive.ucsd.edu/ProteoSAFe/static/massive.jsp>) under the data set identifier MSV000092895.

ADDITIONAL FILES

The following material is available [online](#).

Supplemental Material

Fig. S1 (AAC00850-23-s0001.pdf). SDS-PAGE of insoluble proteins obtained from 42°C incubated culture as positive control (ctrl+), untreated control samples (ctrl), and samples treated for 1, 4, and 24 h by vancomycin and enrofloxacin. The loading volume of each sample was normalized based on the concentration of total protein.

REFERENCES

- Levin-Reisman I, Ronin I, Gefen O, Braniss I, Shoshan N, Balaban NQ. 2017. Antibiotic tolerance facilitates the evolution of resistance. *Science* 355:826–830. <https://doi.org/10.1126/science.aaj2191>
- Bakkeren E, Huisman JS, Fattinger SA, Hausmann A, Furter M, Egli A, Slack E, Sellin ME, Bonhoeffer S, Regoes RR, Diard M, Hardt W-D. 2019. Salmonella persisters promote the spread of antibiotic resistance plasmids in the gut. *Nature* 573:276–280. <https://doi.org/10.1038/s41586-019-1521-8>
- Hobby GL, Meyer K, Chaffee E. 1942. Observations on the mechanism of action of penicillin. *Exper Biol and Med* 50:281–285. <https://doi.org/10.3181/00379727-50-13773>
- Zhang Y. 2014. Persisters, persistent infections and the Yin–Yang model. *Emerg Microbes Infect* 3:e3. <https://doi.org/10.1038/emi.2014.3>
- Urbaniec J, Xu Y, Hu Y, Hingley-Wilson S, McFadden J. 2022. Phenotypic heterogeneity in persisters: a novel ‘hunker’ theory of persistence. *FEMS Microbiol Rev* 46:1–16. <https://doi.org/10.1093/femsre/fuab042>
- Amato SM, Brynildsen MP. 2015. Persister heterogeneity arising from a single metabolic stress. *Curr Biol* 25:2090–2098. <https://doi.org/10.1016/j.cub.2015.06.034>
- Kaldalu N, Hauryliuk V, Tenson T. 2016. Persisters—as elusive as ever. *Appl Microbiol Biotechnol* 100:6545–6553. <https://doi.org/10.1007/s00253-016-7648-8>
- Pacios O, Blasco L, Bleriot I, Fernandez-García L, Ambroa A, López M, Bou G, Cantón R, García-Contreras R, Wood TK, Tomás M. 2020. (p)ppGpp and its role in bacterial persistence: new challenges. *Antimicrob Agents Chemother* 64:e01283-20. <https://doi.org/10.1128/AAC.01283-20>
- Liu S, Brul S, Zaat SAJ. 2020. Bacterial persister-cells and spores in the food chain: their potential inactivation by antimicrobial peptides (amps). *IJMS* 21:8967. <https://doi.org/10.3390/ijms21238967>
- Song S, Wood TK. 2021. Are we really studying persister cells? *Environ Microbiol Rep* 13:3–7. <https://doi.org/10.1111/1758-2229.12849>
- Balaban NQ, Helaine S, Lewis K, Ackermann M, Aldridge B, Andersson DI, Brynildsen MP, Bumann D, Camilli A, Collins JJ, Dehio C, Fortune S, Ghigo J-M, Hardt W-D, Harms A, Heinemann M, Hung DT, Jenal U, Levin BR, Michiels J, Storz G, Tan M-W, Tenson T, Van Melderen L, Zinkernagel A. 2019. Definitions and guidelines for research on antibiotic persistence. *Nat Rev Microbiol* 17:441–448. <https://doi.org/10.1038/s41579-019-0207-4>
- Patel S, Preuss CV, Bernice F. 2022. Vancomycin. In *StatPearls*. StatPearls Publishing: Treasure Island, FL, USA.
- Bhatt S, Chatterjee S. 2022. Fluoroquinolone antibiotics: occurrence, mode of action, resistance, environmental detection, and remediation – a comprehensive review. *Environ Pollut* 315:120440. <https://doi.org/10.1016/j.envpol.2022.120440>
- De Oliveira AP, Watts JL, Salmon SA, Aarestrup FM. 2000. Antimicrobial susceptibility of *Staphylococcus aureus* isolated from bovine mastitis in Europe and the United States. *J Dairy Sci* 83:855–862. [https://doi.org/10.3168/jds.S0022-0302\(00\)74949-6](https://doi.org/10.3168/jds.S0022-0302(00)74949-6)
- Liu S, Laman P, Jensen S, van der Wel NN, Kramer G, Zaat SAJ, Brul S. 2023 Isolation and characterization of persisters of the pathogenic microorganism *Staphylococcus aureus*. *Microbiology*. <https://doi.org/10.1101/2023.09.19.558453>
- Murawski AM, Brynildsen MP. 2021. Ploidy is an important determinant of fluoroquinolone persister survival. *Curr Biol* 31:2039–2050. <https://doi.org/10.1016/j.cub.2021.02.040>
- Wilmaerts D, Focant C, Matthay P, Michiels J. 2022. Transcription-coupled DNA repair underlies variation in persister awakening and the emergence of resistance. *Cell Rep* 38:110427. <https://doi.org/10.1016/j.celrep.2022.110427>
- Vos M. 2009. Why do bacteria engage in homologous recombination? *Trends Microbiol* 17:226–232. <https://doi.org/10.1016/j.tim.2009.03.001>
- Peyrusson F, Varet H, Nguyen TK, Legendre R, Sismeiro O, Coppée J-Y, Wolz C, Tenson T, Van Bambeke F. 2020. Intracellular *Staphylococcus aureus* persists upon antibiotic exposure. *Nat Commun* 11:2200. <https://doi.org/10.1038/s41467-020-15966-7>
- Noor E, Eden E, Milo R, Alon U. 2010. Central carbon metabolism as a minimal biochemical walk between precursors for Biomass and energy. *Mol Cell* 39:809–820. <https://doi.org/10.1016/j.molcel.2010.08.031>
- Sachla AJ, Helmann JD. 2021. Resource sharing between central metabolism and cell envelope synthesis. *Curr Opin Microbiol* 60:34–43. <https://doi.org/10.1016/j.mib.2021.01.015>
- Somerville GA, Chaussee MS, Morgan CI, Fitzgerald JR, Dorward DW, Reitzer LJ, Musser JM. 2002. *Staphylococcus aureus* aconitase inactivation unexpectedly inhibits post-exponential-phase growth and enhances stationary-phase survival. *Infect Immun* 70:6373–6382. <https://doi.org/10.1128/IAI.70.11.6373-6382.2002>
- Kuroda M, Kuroda H, Oshima T, Takeuchi F, Mori H, Hiramatsu K. 2003. Two-component system VraSR positively modulates the regulation of cell-wall biosynthesis pathway in *Staphylococcus aureus*. *Mol Microbiol* 49:807–821. <https://doi.org/10.1046/j.1365-2958.2003.03599.x>
- Soe YM, Bedoui S, Stinear TP, Hachani A. 2021. Intracellular *Staphylococcus aureus* and host cell death pathways. *Cell Microbiol* 23:e13317. <https://doi.org/10.1111/cmi.13317>
- Rudra P, Boyd JM. 2020. Metabolic control of virulence factor production in *Staphylococcus aureus*. *Curr Opin Microbiol* 55:81–87. <https://doi.org/10.1016/j.mib.2020.03.004>
- Goncheva MI, Chin D, Heinrichs DE. 2022. Nucleotide biosynthesis: the base of bacterial pathogenesis. *Trends Microbiol* 30:793–804. <https://doi.org/10.1016/j.tim.2021.12.007>
- Yee R, Cui P, Shi W, Feng J, Zhang Y. 2015. Genetic screen reveals the role of purine metabolism in *Staphylococcus aureus* persistence to rifampicin. *Antibiotics (Basel)* 4:627–642. <https://doi.org/10.3390/antibiotics4040627>
- Jin Q, Xie X, Zhai Y, Zhang H. 2023. Mechanisms of folate metabolism-related substances affecting *Staphylococcus aureus* infection. *Int J Med Microbiol* 313:151577. <https://doi.org/10.1016/j.ijmm.2023.151577>
- Morgan J, Smith M, Mc Auley MT, Enrique Salcedo-Sora J. 2018. Disrupting folate metabolism reduces the capacity of bacteria in exponential growth to develop persisters to antibiotics. *Microbiol* 164:1432–1445. <https://doi.org/10.1099/mic.0.000722>
- Hartl FU, Bracher A, Hayer-Hartl M. 2011. Molecular chaperones in protein folding and proteostasis. *Nature* 475:324–332. <https://doi.org/10.1038/nature10317>
- Savijoki K, Miettinen I, Nyman TA, Kortesoja M, Hanski L, Varmanen P, Fallarero A. 2020. Growth mode and physiological state of cells prior to biofilm formation affect immune evasion and persistence of *Staphylococcus aureus*. *Microorganisms* 8:106. <https://doi.org/10.3390/microorganisms8010106>
- Huemer M, Mairpady Shambat S, Bergada-Pijuan J, Söderholm S, Boumasmoud M, Vulin C, Gómez-Mejía A, Antelo Varela M, Tripathi V, Götschi S, Marques Maggio E, Hasse B, Brugger SD, Bumann D, Schuepbach RA, Zinkernagel AS. 2021. Molecular reprogramming and phenotype switching in *Staphylococcus aureus* lead to high antibiotic persistence and affect therapy success. *Proc Natl Acad Sci U S A* 118:e2014920118. <https://doi.org/10.1073/pnas.2014920118>
- Peyrusson F, Nguyen TK, Najdovski T, Van Bambeke F. 2022. Host cell oxidative stress induces dormant *Staphylococcus aureus* persisters. *Microbiol Spectr* 10:e0231321. <https://doi.org/10.1128/spectrum.02313-21>

34. Frees D, Gerth U, Ingmer H. 2014. Clp chaperones and proteases are central in stress survival, virulence and antibiotic resistance of *Staphylococcus aureus*. *Int J Med Microbiol* 304:142–149. <https://doi.org/10.1016/j.ijmm.2013.11.009>
35. Ju Y, An Q, Zhang Y, Sun K, Bai L, Luo Y. 2021. Recent advances in Clp protease modulation to address virulence, resistance and persistence of MRSA infection. *Drug Discov Today* 26:2190–2197. <https://doi.org/10.1016/j.drudis.2021.05.014>
36. Stahlhut SG, Alqarzaee AA, Jensen C, Fisker NS, Pereira AR, Pinho MG, Thomas VC, Frees D. 2017. The ClpXP protease is dispensable for degradation of unfolded proteins in *Staphylococcus aureus*. *Sci Rep* 7:11739. <https://doi.org/10.1038/s41598-017-12122-y>
37. Frees D, Qazi SNA, Hill PJ, Ingmer H. 2003. Alternative roles of ClpX and ClpP in *Staphylococcus aureus* stress tolerance and virulence. *Mol Microbiol* 48:1565–1578. <https://doi.org/10.1046/j.1365-2958.2003.03524.x>
38. Fourie KR, Wilson HL. 2020. Understanding Groel and DnaK stress response proteins as antigens for bacterial diseases. *Vaccines (Basel)* 8:773. <https://doi.org/10.3390/vaccines8040773>
39. Dawan J, Wei S, Ahn J. 2020. Role of antibiotic stress in phenotypic switching to persister cells of antibiotic-resistant *Staphylococcus aureus*. *Ann Microbiol* 70:1–8. <https://doi.org/10.1186/s13213-020-01552-1>
40. Singh VK, Utaida S, Jackson LS, Jayaswal RK, Wilkinson BJ, Chamberlain NR. 2007. Role for dnaK locus in tolerance of multiple stresses in *Staphylococcus aureus*. *Microbiology (Reading)* 153:3162–3173. <https://doi.org/10.1099/mic.0.2007/009506-0>
41. Keogh RA, Zapf RL, Frey A, Marino EC, Null GG, Wiemels RE, Holzschu DL, Shaw LN, Carroll RK. 2021. *Staphylococcus aureus* trigger factor is involved in biofilm formation and cooperates with the chaperone PpiB. *J Bacteriol* 203:e00681–20. <https://doi.org/10.1128/JB.00681-20>
42. Michalik S, Depke M, Murr A, Gesell Salazar M, Kusebauch U, Sun Z, Meyer TC, Surmann K, Pfortner H, Hildebrandt P, Weiss S, Palma Medina LM, Gutjahr M, Hammer E, Becher D, Pribyl T, Hammerschmidt S, Deutsch EW, Bader SL, Hecker M, Moritz RL, Mäder U, Völker U, Schmidt F. 2017. A global *Staphylococcus aureus* proteome resource applied to the *in vivo* characterization of host-pathogen interactions. *Sci Rep* 7:9718. <https://doi.org/10.1038/s41598-017-10059-w>
43. Jarick M, Bertsche U, Stahl M, Schultz D, Methling K, Lalk M, Stigloher C, Mirco Steger AK. 2009. Localization studies of the FemXAB protein family in *Staphylococcus aureus*. *Sci Rep*:13693.
44. Zhou J, Cai Y, Liu Y, An H, Deng K, Ashraf MA, Zou L, Wang J. 2022. Breaking down the cell wall: still an attractive antibacterial strategy. *Front Microbiol* 13:952633. <https://doi.org/10.3389/fmicb.2022.952633>
45. Tajbakhsh G, Golemi-Kotra D. 2019. The Dimerization interface in VraR is essential for induction of the cell wall stress response in *Staphylococcus aureus*: a potential druggable target. *BMC Microbiol* 19:153. <https://doi.org/10.1186/s12866-019-1529-0>
46. Wilmaerts D, Windels EM, Verstraeten N, Michiels J. 2019. General mechanisms leading to persister formation and awakening. *Trends Genet* 35:401–411. <https://doi.org/10.1016/j.tig.2019.03.007>
47. Qu X, Lancaster L, Noller HF, Bustamante C, Tinoco I. 2012. Ribosomal protein S1 unwinds double-stranded RNA in multiple steps. *Proc Natl Acad Sci U S A* 109:14458–14463. <https://doi.org/10.1073/pnas.1208950109>
48. Wilson DN, Nierhaus KH. 2005. Ribosomal proteins in the spotlight. *Crit Rev Biochem Mol Biol* 40:243–267. <https://doi.org/10.1080/10409230500256523>
49. Ha KP, Edwards AM. 2021. DNA repair in *Staphylococcus aureus*. *Microbiol Mol Biol Rev* 85:e0009121.
50. Du H, Zhou L, Lu Z, Bie X, Zhao H, Niu YD, Lu F. 2020. Transcriptomic and proteomic profiling response of methicillin-resistant *Staphylococcus aureus* (MRSA) to a novel bacteriocin, plantaricin GZ1-27 and its inhibition of biofilm formation. *Appl Microbiol Biotechnol* 104:7957–7970. <https://doi.org/10.1007/s00253-020-10589-w>
51. McHenry CS. 2011. Bacterial replicases and related polymerases. *Curr Opin Chem Biol* 15:587–594. <https://doi.org/10.1016/j.cbpa.2011.07.018>
52. Hernández-Tamayo R, Oviedo-Bocanegra LM, Fritz G, Graumann PL. 2019. Symmetric activity of DNA polymerases at and recruitment of exonuclease ExoR and of PolA to the *Bacillus subtilis* replication Forks. *Nucleic Acids Res* 47:8521–8536. <https://doi.org/10.1093/nar/gkz554>
53. Podlesek Z, Žgur Bertok D. 2020. The DNA damage inducible SOS response is a key player in the generation of bacterial Persister cells and population wide tolerance. *Front Microbiol* 11:1785. <https://doi.org/10.3389/fmicb.2020.01785>
54. Kaushik V, Tiwari M, Tiwari V. 2022. Interaction of RecA mediated SOS response with bacterial persistence, biofilm formation, and host response. *Int J Biol Macromol* 217:931–943. <https://doi.org/10.1016/j.ijbiomac.2022.07.176>
55. Bollen C, Dewachter L, Michiels J. 2021. Protein aggregation as a bacterial strategy to survive antibiotic treatment. *Front Mol Biosci* 8:669664. <https://doi.org/10.3389/fmolb.2021.669664>
56. Wood TK, Song S, Yamasaki R. 2019. Ribosome dependence of persister cell formation and resuscitation. *J Microbiol* 57:213–219. <https://doi.org/10.1007/s12275-019-8629-2>
57. Frank MW, Whaley SG, Rock CO. 2021. Branched-chain amino acid metabolism controls membrane phospholipid structure in *Staphylococcus aureus*. *J Biol Chem* 297:101255. <https://doi.org/10.1016/j.jbc.2021.101255>
58. Belcheva A, Verma V, Korenevsky A, Fridman M, Kumar K, Golemi-Kotra D. 2012. Roles of DNA sequence and sigma A factor in transcription of the *vraSR* operon. *J Bacteriol* 194:61–71. <https://doi.org/10.1128/JB.06143-11>
59. Severin A, Wu SW, Tabei K, Tomasz A. 2004. Penicillin-binding protein 2 is essential for expression of high-level vancomycin resistance and cell wall synthesis in vancomycin-resistant *Staphylococcus aureus* carrying the enterococcal *vanA* gene complex. *Antimicrob Agents Chemother* 48:4566–4573. <https://doi.org/10.1128/AAC.48.12.4566-4573.2004>
60. Crane JK, Alvarado CL, Sutton MD. 2021. Role of the SOS response in the generation of antibiotic resistance *in vivo*. *Antimicrob Agents Chemother* 65:e0001321. <https://doi.org/10.1128/AAC.00013-21>
61. Zheng EJ, Stokes JM, Collins JJ. 2020. Eradicating bacterial persisters with combinations of strongly and weakly metabolism-dependent antibiotics. *Cell Chem Biol* 27:1544–1552. <https://doi.org/10.1016/j.chembiol.2020.08.015>
62. Liu S, Brul S, Zaat SAJ. 2021. Isolation of persister cells of *Bacillus subtilis* and determination of their susceptibility to antimicrobial peptides. *IJMS* 22:10059. <https://doi.org/10.3390/ijms221810059>
63. Liebeke M, Dörries K, Meyer H, Lalk M. 2012. Metabolome analysis of gram-positive bacteria such as *Staphylococcus aureus* by GC-MS and LC-MS. *Methods Mol Biol* 815:377–398. https://doi.org/10.1007/978-1-61779-424-7_28
64. Tyanova S, Temu T, Sinitcyn P, Carlson A, Hein MY, Geiger T, Mann M, Cox J. 2016. The perseus computational platform for comprehensive analysis of (prote)omics data. *Nat Methods* 13:731–740. <https://doi.org/10.1038/nmeth.3901>
65. Bu D, Luo H, Huo P, Wang Z, Zhang S, He Z, Wu Y, Zhao L, Liu J, Guo J, Fang S, Cao W, Yi L, Zhao Y, Kong L. 2021. KOBAS-i: intelligent prioritization and exploratory visualization of biological functions for gene enrichment analysis. *Nucleic Acids Res* 49:W317–W325. <https://doi.org/10.1093/nar/gkab447>
66. López-Ibáñez J, Pazos F, Chagoyen M. 2016. MBROLE 2.0—functional enrichment of chemical compounds. *Nucleic Acids Res* 44:W201–4. <https://doi.org/10.1093/nar/gkw253>